Pharmacophore modeling, virtual screening, docking and *in silico* ADMET analysis of protein kinase B (PKB β) inhibitors

Vivek K. Vyas*, Manjunath Ghate, Ashutosh Goel

Department of Pharmaceutical Chemistry, Institute of Pharmacy, Nirma University, Ahmedabad 382 481, Gujarat, India

ARTICLE INFO

ABSTRACT

Protein kinase B (PKB) is a key mediator of proliferation and survival pathways that are critical for cancer growth. Therefore, inhibitors of PKB are useful agents for the treatment of cancer. Herein, we describe pharmacophore-based virtual screening combined with docking study as a rational strategy for identification of novel hits or leads. Pharmacophore models of PKB β inhibitors were established using the DISCOtech and refined with GASP from compounds with IC_{50} values ranging from 2.2 to 246 nM. The best pharmacophore model consists of one hydrogen bond acceptor (HBA), one hydrogen bond donor (HBD) site and two hydrophobic (HY) features. The pharmacophore models were validated through receiver operating characteristic (ROC) and Güner-Henry (GH) scoring methods indicated that the model-3 was statistically valuable and reliable in identifying PKB β inhibitors. Pharmacophore model as a 3D search query was searched against NCI database. Several compounds with different structures (scaffolds) were retrieved as hits. Molecules with a Q_{fit} value of more than 95 and three other known inhibitors were docked in the active site of PKB to further explore the binding mode of these compounds. Finally *in silico* pharmacokinetic and toxicities were predicted for active hit molecules. The hits reported here showed good potential to be PKB β inhibitors.

© 2013 Elsevier Inc. All rights reserved.

1. Introduction

The phosphoinositide 3-kinase (PI3-K) family of enzymes has a central function in regulating variety of cellular processes as metabolism, cell growth, proliferation, apoptosis and chemotaxis [1]. The serine/threonine protein kinase B (PKB, also known as Akt) is a central point in PI3-K cascade. PKB phosphorylate a plethora of substrates and coupling PI3-K with the mammalian target of rapamycin (mTOR). PKB is a key downstream component in the PI3-K signaling pathway [2] and has an ability to phosphorylate and change the activity of many critical metabolic targets. There are three human isoforms of PKB known as PKB-α, -β, -γ or Akt-1, -2, -3. These three isoforms of PKB shares a common structure made up of three domains: the N-terminal pleckstrin homology (PH) domain binds phosphatidylinositol-3,4,5-triphosphate (PI(3,4,5)P₃) and, is essential in the activation of the enzyme, a catalytic kinase domain related to other AGC (protein kinase A, protein kinase G and protein kinase C) family kinases, contains a classical kinase ATP-binding site and a hydrophobic motif (HM) at the C-terminal, which forms

a docking site for phosphoinositide-dependent kinase 1 (PDK1) [3]. Activation of PI3-K upon binding of ligand to receptor tyrosine kinase (RTK) at the cell surface produces PI(3,4,5)P₃. Binding of PKB to PI(3,4,5)P₃ through the PH domain of the enzyme promotes activation of the kinase by phosphorylation on Ser473 and Thr308 [4,5]. Activated PKB inhibits apoptosis and stimulates cell cycle progression by phosphorylating numerous targets in various cell types, including cancer cells. PKB is the most significant mediator of the PI3-K signaling cascade and is localized to the membrane by interactions between its PH domain and PI(3,4,5)P₃. Upstream RTK, the lipid kinase PI3-K and PKB itself, particularly the β-isoform, are commonly amplified or mutated at the genetic level, over-expressed, or over-activated in human tumors particularly in breast, ovarian and cervical carcinoma [6]. The lipid phosphatase PTEN (phosphatase and tensin homolog) is a negative regulator of PKB that dephosphorylates PI(3,4,5)P₃ and deactivates PKB. Over-expression of PKB as a result in inactivation of tumor suppressor PTEN has been correlated with an increasing number of human cancers [7]. Deletion of PTEN is frequently observed in human tumors, especially glioblastoma, endometrial, and prostate cancers [8,1]. The prevalence of PKB activity is the hallmark of several aggressive malignancies, as a result, PKB has emerged as an attractive target for the development of novel anticancer therapeutics [9]. The development of inhibitors of PKB as

small molecule is a valuable approach for anticancer drug discovery.

There are three strategies can be applied for the development of novel PKB inhibitors, targeting toward pleckstrin homology (PH) domain [10], ATP-binding kinase domain [11], or and hinge-region domain [12]. In contrast to the above strategies, there has been increased interest in developing PKB inhibitors that specifically target the substrate binding groove adjacent to the ATP-binding site. Several publications in this area reported many different classes of ATP-competitive small molecule inhibitors of PKB [13–17]. Poor oral bioavailability and short half-life in animals are the main problem of this kind of compounds (GSK690693) as a clinical agent [18]. However, only limited number of compounds entered into early phase of clinical trials [19]. Therefore, challenges remain for the development of selective ATP-competitive inhibitors of PKB as a suitable drug candidate. Pharmacophore mapping, virtual screening and docking are the rational methods for identification of novel hits or leads with diverse chemical scaffolds [20–24]. A pharmacophore can be considered as the ensemble of steric and electrostatic features of different compounds which are necessary to ensure optimal supramolecular interactions with a specific biological target structure and to trigger or to block its biological response. Molecular docking is widely used to suggest the binding modes of protein inhibitors. *In silico* pharmacokinetic and toxicity prediction play an important role in drug discovery and development because ADMET (absorption, distribution, metabolism and excretion and toxicity) is a major cause of failure of drug candidates during late phases of drug development [25]. The present study was undertaken to explore key structural requirements for PKB β inhibition utilizing combination of the above modeling methods for the design of novel, potent and selective PKB β inhibitors.

2. Materials and methods

2.1. Dataset

The available data set of 73 compounds (Table A under Supplementary Materials) were obtained from the literature [26–28], consisted of 4-amino-1-(7*H*-pyrrolo[2,3-*d*]pyrimidin-4-yl)piperidine-4-carboxamides (41 compounds), [26] 4-(4-aminopiperidin-1-yl)-7*H*-pyrrolo[2,3-*d*]pyrimidines (23 compounds) [27] and 6-phenylpurine (9 compounds) [28]. PKB β IC_{50} values were measured [26–28] by inhibition of PKB β kinase activity in a radiometric filter binding assay which employed similar experimental conditions and procedures.

2.2. Computational details

The pharmacophore mapping, database searching and molecular docking study were performed using the SYBYL X 1.2 software from Tripos Inc., St. Louis, MO, USA [29]. All the compounds were sketched using SKETCH function of SYBYL. Partial atomic charges were calculated by the Gasteiger–Huckel method and energy minimizations were performed using the Tripos force field [30] with a distance-dependent dielectric and the Powell conjugate gradient algorithm convergence criterion of 0.01 kcal/mol Å [31].

2.3. Generation of pharmacophore models

The first step in building a pharmacophore model from a set of ligands is the alignment of the molecules, including position, rotation and conformation. Twelve molecules (Fig. 1) were selected to generate 10 pharmacophore models using DISCOtech, based on chemical diversity. The genetic algorithm similarity program (GASP) was used to refine the generated model (4 models) which

uses a genetic algorithm to identify common feature of different molecules. A pharmacophore contains essential features like hydrogen bond donor, hydrogen bond acceptor, hydrophobic, etc. Chemical structures of molecules used in pharmacophore mapping are shown in Fig. 1. All the parameters were kept as default except population size (125), mutation weight (96), fitness increment (0.02) and number of alignment (04) [32].

2.4. Validation of the pharmacophore model

In order to evaluate the reliability and accuracy of the generated 3D pharmacophore models, model 1–4 were validated by receiver operating characteristic (ROC) and Güner-Henry (GH) scoring methods.

2.4.1. Receiver operating characteristic (ROC) analysis

Models 1–4 were validated by assessing their ability to selectively capture diverse PKB β inhibitors from a large list of decoys (molecules which are presumably inactive against the examined target) employing ROC analysis [33]. Therefore, it was necessary to prepare valid evaluation structural database (testing set) that contains an appropriate list of decoy compounds in combination with diverse list of known active compounds. Active testing compounds were defined as those possessing PKB β (IC_{50} values) ranging from 2.5 nm to 250 nm. The testing set included 33 active compounds along with their 20 conformers generated using a genetic algorithm-based global optimizer to find the low energy conformations of a molecule. A total of 660 conformers of 33 compounds constitute a test set. The ROC curve is a function of Sp *versus* the Se, and the area under the ROC curve (AUC) value is the important way of measuring the performance of the test.

$$Se = \frac{TP}{TP + FN}$$

where TP is the number of true positive compounds, FN is the number of false negative compounds.

$$Sp = \frac{FP}{TN + FP}$$

where TN is the number of true negative compounds, FP is the number of false positive compounds.

The ROC curve is a graphical plot of the true positive rate (Se) *versus* false positive rate $(1 - Sp)$, and the area under the ROC curve (AUC) is the important way of measuring the performance of the test.

$$AUC = \sum_{X=2}^{N} Se(x)[(1 - Sp)(x) - (1 - Sp)(x - 1)],$$

where $Se(x)$ is the percent of the true positives *versus* the total positives at rank position x, $(1 - Sp)(x)$ is the percent of the false positives *versus* the total negatives at rank position x.

2.4.2. Güner-Henry (GH) scoring method

The GH score has been successfully applied to quantify model selectivity (best model), accuracy of hits and the recall of actives from a molecule dataset consisting of known actives and inactives. GH scoring methodology has been successfully applied for quantification of model selectivity and coverage of activity space from database mining [34] and for the evaluation of the effectiveness of similarity search in databases containing both structural and biological activity data [35]. The GH score contains a coefficient to penalize excessive hit list size and, when evaluating hit lists, is calibrated by weighting the score with respect to the yield and coverage. The GH score ranges from 0, which indicates the null model, to 1, which indicates the ideal model (*i.e.*, containing all of, and
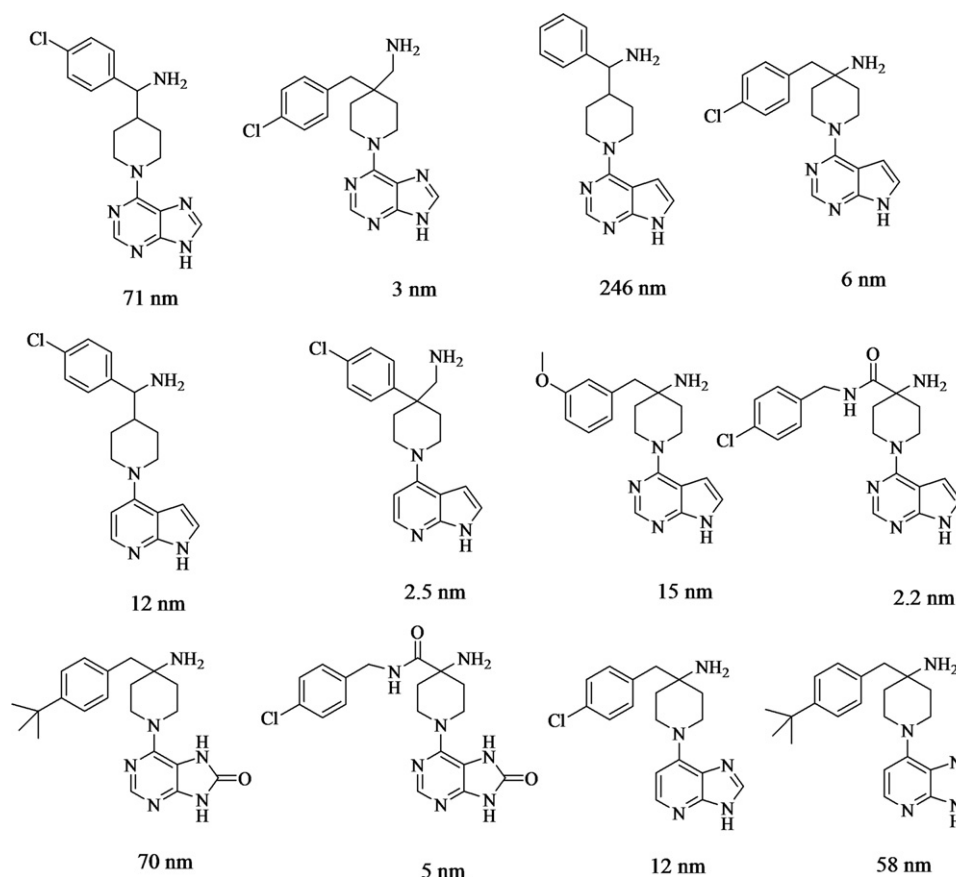
Fig. 1. Chemical structures of the 12 compounds used to generate pharmacophore model using DISCOtech/GASP with PKB β inhibitory activity ranging from 2.2 to 246 nM.

only, the active ligands). The GH value is expected to be greater than 0.7 [36]. It is considered a relevant metric, as it takes into account both the percent yield of actives in a database (%Y, recall) and the percent ratio of actives in the hit list (%A, precision). The GH scoring formula can be applied to identify best tolerance for an analysis testing different RMS tolerance in fixed atomic position. For fixed positions tolerance an optimum GH score can be calculated. This method can also be applied to calculate highest GH score for the activity of a class of compounds clustered in a group. Hence, using the GH score method for each cluster of compounds aimed for particular activity, one can associate ownership for each cluster. The GH scoring method was applied to the previously mentioned 33 known inhibitors of PKB β with their 660 conformers and the decoy dataset molecules to validate the pharmacophore models. The GH analysis was done by computing the following variables: (a) the percent active (%A), which represents the coverage of activity space by the model, (b) the percent yield (%Y), which is a measure of the selectivity of the model, (c) the enrichment factor (E), and (d) the GH score. These variables are determined using information derived from the total number of compounds in the drug database (D), the number of actives in the database (A), the number of actives retrieved by the model (Ha), and the total number of hits retrieved by the model (Ht).

$$\%A = \frac{Ha}{A} \times 100$$

$$\%Y = \frac{Ha}{Ht} \times 100$$

$$E = (Ha/Ht)/(A/D)$$

$$GH = \frac{Ha(3A + Ht)}{4HtA}\left(1 - \frac{Ht - Ha}{D - A}\right)$$

2.5. Virtual screening

Pharmacophore-based virtual screening can be efficiently used to find novel potential leads for further development from a virtual database. After 3D pharmacophore model generation and validation the best pharmacophore model was used as a 3D search query for retrieving potent molecules from the NCI chemical database with novel chemical structures and desired chemical features, and to locate the appropriate binding orientations and conformations of these substructures with PKB β. The hits identified from NCI database were filtered by applying Lipinski's rule-of-five [37] that sets the criteria for drug-like properties. Molecules which satisfied all the features of the pharmacophore model used as the 3D query were retained as hits.

2.6. Molecular docking

The Surflex–Dock module of SYBYL was used for molecular docking. The X-ray crystallographic structures of PKB β solved at 1.8 Å complex with ligand [PDB: 2JDO] [38] was taken from the protein data bank (PDB) and modified for docking calculations. Co-crystallized ligand was removed from the structure, water molecules were removed, H atoms were added and side chains were fixed during protein preparation. Protein structure minimization was performed by applying Tripos force field and partial atomic charges were calculated by Gasteiger–Huckel method.

Table 1
Result of pharmacophore hypothesis generated using DISCOtech and refined by GASP.

Model	Fitness score	Size	Hits	Dmean	Features
1	3450.04	4	12	3.04	DS1, AA1, HY1, HY2
2	3468.98	4	12	3.04	DS1, AA1, HY1, HY2
3	3428.57	4	12	3.04	DS1, AA1, HY1, HY2
4	3456.41	4	12	3.04	DS1, AA1, HY1, HY2

Size is total number of features in the models; Hits is number of molecules that matched during the search; Dmean is average inter-point distance between the features; DS1 represent one donor feature in pharmacophore models; AA1 represent one hydrogen bond acceptor atom in models; HY1 and HY2 represent hydrophobic features in the models

2.7. In silico ADMET studies

In silico pharmacokinetic properties and toxicities were predicted using OSIRIS property explorer which uses Chou and Jurs algorithm, based on computed atom contributions [39].

3. Results and discussion

3.1. Results of pharmacophore mapping

In order to build pharmacophore models, we have searched the literature for many structurally diverse compounds as PKB β inhibitors, however the fact that pharmacophore mapping require the training set compounds should be assayed by a single bioassay procedure restricted us to certain published literature [26–28] on PKB β inhibitors. A total of 73 compounds were used in this study (Table A under Supplementary Materials). The biological activity in the training subsets spanned from 2.2 to 110,000 nM. DISCOtech derived ten chemical-feature-based pharmacophore hypotheses which were further refined using GASP module. GASP generated four refined models and, among these models, model-3 was considered as the best one characterized by the highest AUC value and better GH score. The four hypotheses generated have a fitness scores ranging from 3428.57 to 3468.98. The fitness score is an overall measure of fit and of overlap volume for the entire collection of structures, and is best considered a tool for assessing convergence of the calculation. The result of the pharmacophore hypothesis is shown in Table 1. A two dimensional pharmacophore hypothesis is shown in Fig. 2. Model-3 contains 1 donor sites, 1 acceptor atom and 2 hydrophobic regions. Pharmacophore mapping results suggested that the presences of four features are essential for good activity of the compounds. The pyrrolo-pyrimidine ring in the molecules is recognized as hydrophobic, and the protonated nitrogen atom of
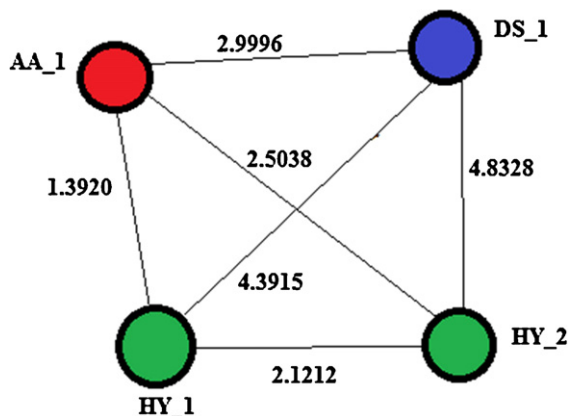

Fig. 2. Two dimensional pharmacophore hypothesis: AA_1 = acceptor atom; DS_1 = donor site; HY_1 = hydrophobic site, HY_2 = hydrophobic site.

Table 2
ROC performances of pharmacophore models as 3D search queries.

Model	ROC-AUC	ACC	SPC	TPR	FNR	Std. error
1	0.65	0.97	0.88	0.99	0.01	0.06
2	0.74	0.97	0.87	0.99	0.01	0.05
3	0.78	0.97	0.87	1	0.0	0.05
4	0.74	0.97	0.88	0.99	0.01	0.05

ROC, receiver operating characteristic; AUC, area under the curve; ACC, overall accuracy; SPC, overall specificity; TPR, overall true positive rate; FNR, overall false negative rate.

pyrole or imidazole ring is recognized as hydrogen bond donor in all hypotheses.

3.2. Pharmacophore model examination

3.2.1. Receiver operating characteristic (ROC) studies

To validate the resulting pharmacophore models, we subjected our pharmacophores to receiver operating curve (ROC) analysis to assess their abilities to correctly classify a list of compounds as active or inactive. In this case, the validity of a particular pharmacophore is indicated by the area under the curve (AUC) of the corresponding ROC curve, as well as the overall accuracy, specificity, true positive rate and false negative rate of the pharmacophore. Table 2 and Fig. 3 show the ROC performances of all pharmacophores models (1–4). In ROC study, model-3 was considered as best model for picking up active molecules in the database, a spiked database including 200 inactive compounds and 33 known inhibitors (660 active conformers). The AUC of ROC curve of model-3 was 0.78 and overall accuracy (ACC) was 0.97 against the randomly selection value of "0.5", demonstrating the reliability of model-3 which might be valuable in identifying diverse compounds with PKB β inhibitory activity.

3.2.2. Güner-Henry (GH) studies

Selection of the best hypotheses was also performed using the Güner-Henry (GH) scoring method. The GH analysis was done by computing the following variables: (a) %A is the percentage of known active compounds retrieved from the database (precision), (b) Ha is the number of actives in the hit list (true positives), (c) A is the number of active compounds in the database, (d) %Y, the percentage of known actives in the hit list (recall), (e) Ht is the number of hits retrieved, (f) D is the number of compounds in the database, (e) E is the enrichment of the concentration of actives by the model relative to random screening without any pharmacophoric approach and (f) GH is the Güner-Henry score. Model-3 succeeded in retrieving 90% of the active compounds, and an enrichment factor of 5.88 and a GH score of 0.83 indicated the good quality of the model (Table 3).

3.3. Virtual screening analysis

Best pharmacophore hypothesis was employed as a 3D search query against the NCI database. Compounds which had their chemical groups spatially overlap (map) with corresponding features of the particular pharmacophoric model were captured as hits. A total number of 24,170 molecules were obtained after substructure searching from databases. These molecules were again screened for drug like compounds by applying Lipinski's rule of five and finally 9829 (see HITS under Supplementary Materials) compounds were obtained which might be useful in rational design of new PKB β inhibitors. The stepwise description of screening procedure is shown in Table B under Supplementary Materials. Molecular docking analyses were carried out with 10 molecules having Q_{fit} value of more than 95 (Fig. 4) to reduce the rate of false positive. The Q_{fit} score represents how close the ligand atoms matched with the
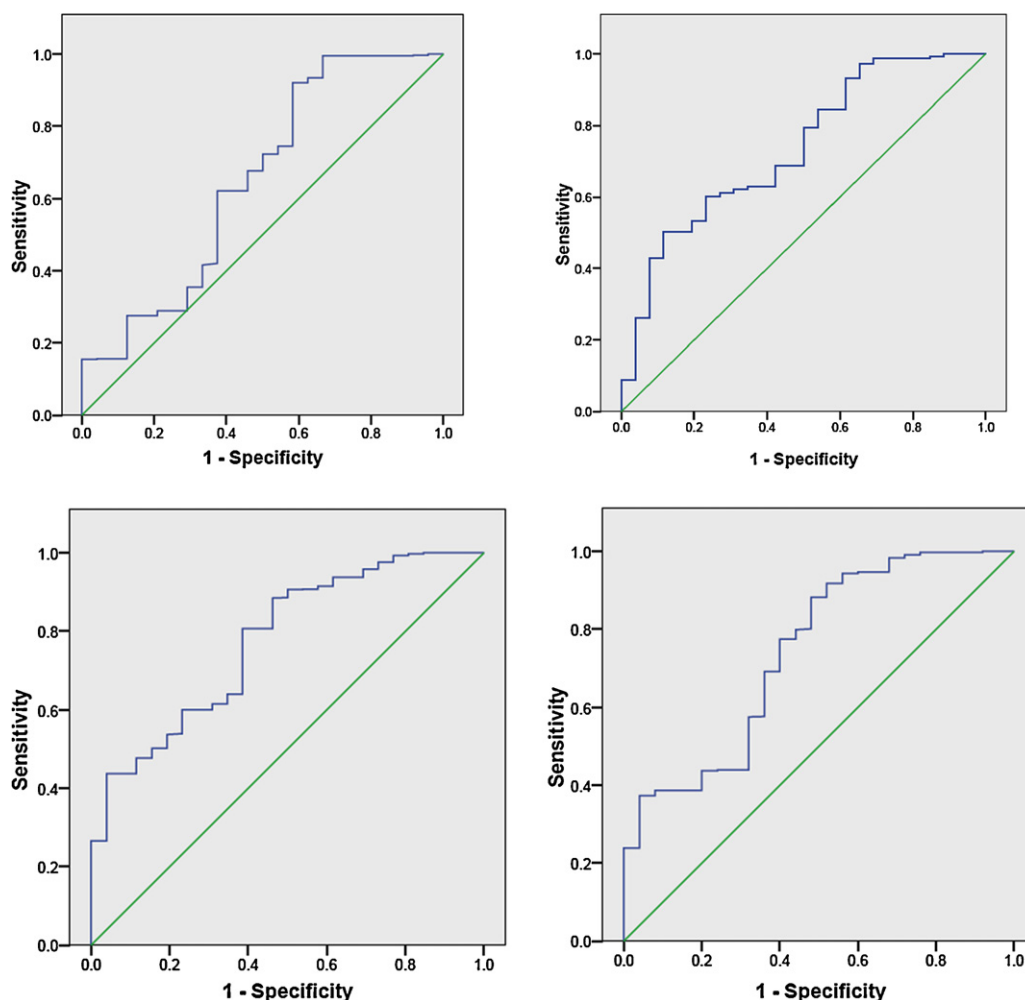
Fig. 3. Receiver operating characteristic (ROC) curves of pharmacophore models.

3D search query. Q_{fit} score is a value between 0 and 100, where a value of 100 is considered as the best. Since that pharmacophore mapping and molecular docking can be synergistically integrated to improve the drug design and development process.

3.4. Molecular docking analysis

To study the binding modes of the active hit molecules with the PKB β enzyme, we performed molecular docking experiments (Table C under Supplementary Materials) into the ligand binding site of the enzyme. In order to validate the docking results known PKB β inhibitors GSK630693 and two other highest active molecules (19 and 59) (Table A under Supplementary Materials) were also docked in the binding site of the enzyme using the Surflex–Dock module. The Surflex–Dock uses an empirically derived scoring function that is based on the binding affinities of protein–ligand complexes and on their X-ray structures.

Protomol represents interaction of ligand with binding site of protein. The protomol is a unique and important factor of the docking algorithm and is a computational representation of assumed ligands that interact with the binding site. Surflex–Dock's scoring function contains hydrophobic, polar, repulsive, entropic, and solvation terms. The co-crystal structure of human PKB β was retrieved from the protein data bank. After running Surflex–Dock, the scores of the active docked conformers were ranked in a molecular spread sheet. We selected the best total score conformers and speculated regarding the detailed binding patterns in the cavity. Surflex–Dock results mainly contain 3 information, total score which is the total Surflex–Dock score expressed as $-\log (K_d)$ to represent binding affinities which include hydrophobic, polar, repulsive, entropic and solvation. Crash value is the degree of inappropriate penetration by the ligand into the protein and of interpenetration between ligand atoms (self-clash) that are separated by rotatable bonds. Crash scores close to 0 are

Table 3
Pharmacophore model evaluation based on the Güner-Henry (GH) scoring method.

Model	%A	%Y	E	GH	D	A	Ht	Ha
1	87.87	69.04	4.89	0.69	233	33	42	29
2	78.78	65.00	4.64	0.64	233	33	40	26
3	90.90	83.33	5.88	0.83	233	33	36	30
4	87.87	72.50	5.12	0.72	233	33	40	29

Ht is number of hits retrieved, Ha is number of actives in hit list, D is number of compounds in a database, %A is a ratio of actives retrieved in hit list, %Y is a fractions of hits relative to size of database (hit rate or selectivity), E is enrichment of active bin by model relative to random screening is GH is Güner-Henry score.
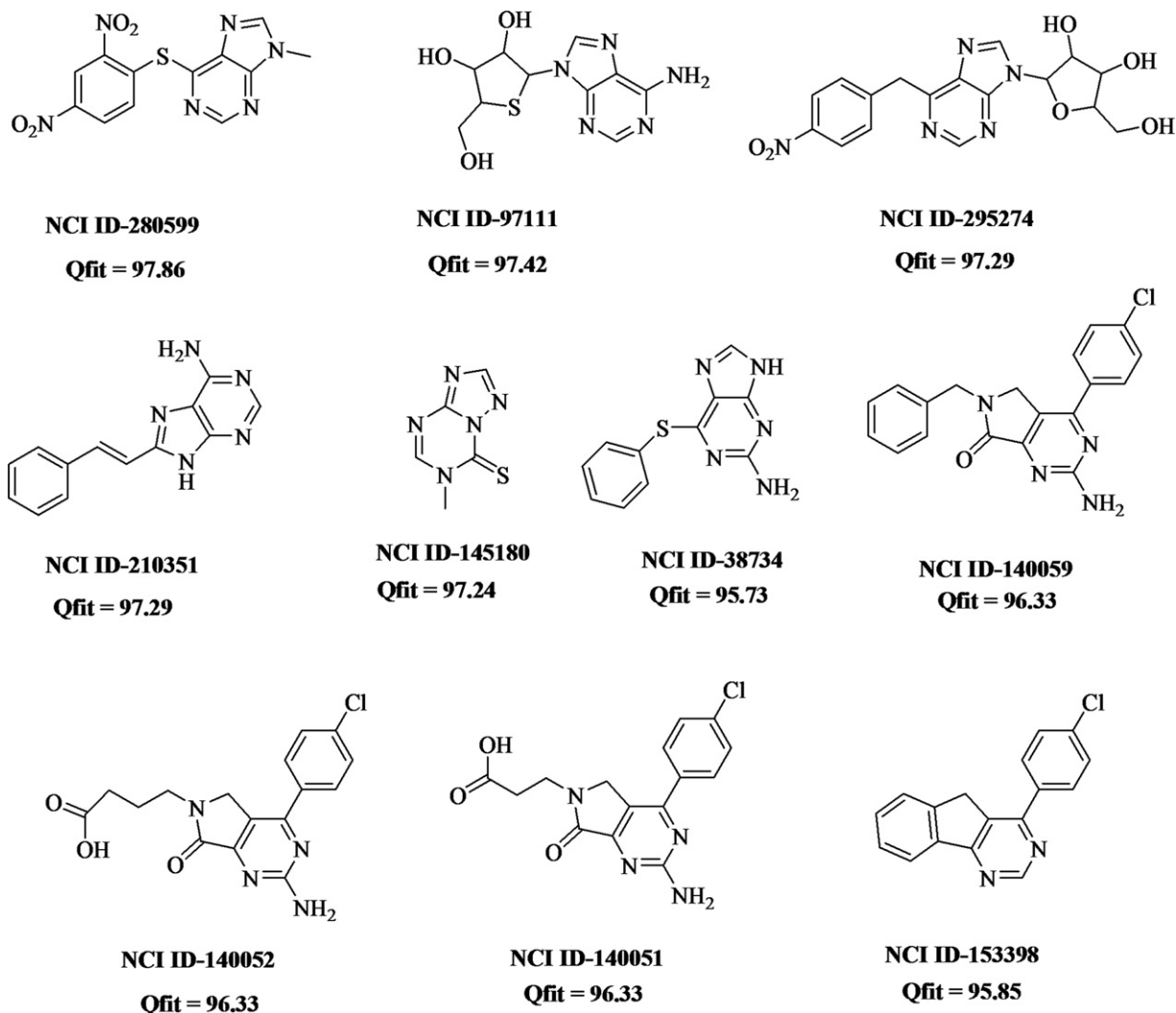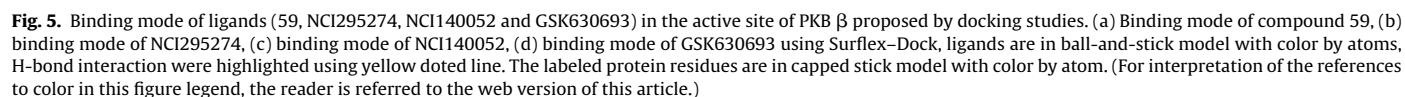
NCI ID-280599

Qfit = 97.86

NCI ID-97111

Qfit = 97.42

NCI ID-295274

Qfit = 97.29

NCI ID-210351

Qfit = 97.29

NCI ID-145180

Qfit = 97.24

NCI ID-38734

Qfit = 95.73

NCI ID-140059

Qfit = 96.33

NCI ID-140052

Qfit = 96.33

NCI ID-140051

Qfit = 96.33

NCI ID-153398

Qfit = 95.85

Fig. 4. Structures of molecules retrieved from NCI database with their Q_{fit} values.

favorable. Polar value is a contribution of the hydrogen bonding and salt bridge interactions to the total score. The polar score may be useful for excluding docking results that make no hydrogen bonds.

3.5. Binding pose of compounds in PKB β

Docking results suggested that compound 59, NCI295274, NCI140052 and GSK630693 [18] have good docking score (Table C under Supplementary Materials). The overall binding of 59, NCI295274, NCI140052 and GSK630693 in PKB β is illustrated in Fig. 5. Docking results showed that compound 59 has highest total score of 8.57. Compound 59 formed three H-bonds with PKB β (Fig. 5a). The nitrogen atom of −NH$_2$ group of ligand formed one H-bond with hydrogen of −NH$_2$ of Arg6 (H$_2$N⋯Arg6, 2.31 Å). Second H-bond was formed between 3 N atom of purine ring with hydrogen atom of amide of Ala232 (purine ring 3N⋯Ala232, 3.14 Å), and third H-bond was formed between hydrogen atom of 5 N (purine ring) with carbonyl oxygen atom of Glu230 (N−H⋯O=C Glu230, 1.95 Å). Docking result showed that NCI295274 has second highest total score of 8.05. Five H-bonds were formed between ligand (NCI295274) and protein (PKB β) (Fig. 5b). The nitro group on benzyl ring formed three H-bonds with −NH$_2$ of Ser9 (N=O⋯Ser9, 2.01 Å; O$_2$N⋯Ser9 2.49 Å; N−O⋯Ser9, 2.21 Å), and one oxygen atom

of −NO$_2$ formed H-bond with −NH$_2$ of Lys277 (N=O⋯Lys277, 1.94 Å). The hydrophobic benzyl ring is in contact with Leu296 and Phe443 which seems to be important residues for binding of ligand in the active site of PKB β. The oxygen atom of hydroxylmethyl group substituted on tetrahydrofuran moiety of NCI295274 formed H-bond with −NH$_2$ of Ala232 (HO⋯Ala232, 1.92 Å). NCI140052 (total score is 7.46) also formed three hydrogen bonds with protein (PKB β) (Fig. 5c). Oxygen atom (hydroxyl) of butanoic acid formed two H-bonds, one with -NH$_2$ of Thr162 (HO⋯Thr162, 2.57 Å) and another with –NH$_2$ of Phe162 (HO⋯Phe162, 1.88 Å). The oxygen atom of (7-oxo) 3,4-dehydropyrrolo moiety of NCI140052 formed H-bond with −NH$_2$ of Lys181 (C=O⋯Lys181, 1.96 Å). The hydrophobic chlorophenyl ring is in contact with Leu155. The overall binding of GSK630693 is illustrated in Fig. 5d. GSK630693 formed three H-bonds with PKB β enzyme (total score is 6.75). Two H-bonds were formed between −NH$_2$ group substituted on oxadiazole ring of GSK630693 and PKB β (H$_2$N⋯HNHArg6, 2.52 Å) (HNH⋯O−C Glu236, 2.75 Å). One H-bond was formed between hydrogen atom of −OH of methylbutanol and Glu230 (O−H⋯O=C Glu230, 2.02 Å). The docking results clearly showed that Glu230 and Arg6 are important amino acids for binding with the known PKB β inhibitors. Ala232 is a common amino acid in binding with active hit NCI295274 and known PKB β inhibitor (compound 59).

Fig. 5. Binding mode of ligands (59, NCI295274, NCI140052 and GSK630693) in the active site of PKB β proposed by docking studies. (a) Binding mode of compound 59, (b) binding mode of NCI295274, (c) binding mode of NCI140052, (d) binding mode of GSK630693 using Surflex–Dock, ligands are in ball-and-stick model with color by atoms, H-bond interaction were highlighted using yellow doted line. The labeled protein residues are in capped stick model with color by atom. (For interpretation of the references to color in this figure legend, the reader is referred to the web version of this article.)

3.6. In silico ADMET analysis

Pharmacokinetic properties and toxicities were predicted for NCI295274 and NCI140052. Results of pharmacokinetic properties and toxicity analysis are shown in Table 4. Solubility and partition coefficient were calculated for pharmacokinetic property while for toxicity study, mutagenicity, tumorigenicity, irritation effect and risk of reproductive effect were predicted. Results of *in silico* pharmacokinetic and toxicity study showed good pharmacokinetic properties. The log *P* value was predicted to determine
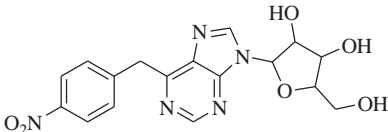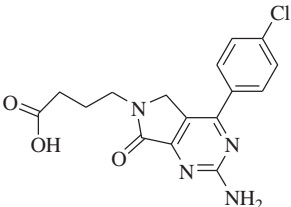
Table 4
In silico ADMET prediction of active hit molecules with best docking score.

Physicochemical and ADMET parameters/ properties	NCI295274 (2-(6-(4-nitrobenzyl)-9H-purin-9-yl)-5-(hydroxymethyl)-tetrahydrofuran-3,4-diol)	NCI140052 (4-(2-amino-4-(4-chlorophenyl)-7-oxo-5H-pyrrolo[3,4-d]pyrimidin-6(7H)-yl)butanoic acid)
Chemical structure		
Mutagenicity	No	Medium risk
Tumorigenicity	No	No
Irritant	No	No
Reproductive effective	No	No
cLog P	0.08	1.6
Solubility	−3.92	−3.69
Molecular weight	387	346
Drug likeness	−18.15	3.1
Drug score	0.39	0.64

Table 5
Contribution of different physicochemical and ADMET parameters/properties on drug score of NCI295274 and NCI140052.

Drug score form of physicochemical and ADMET parameters/properties	NCI295274	NCI140052
cLog P	0.99	0.97
Log S	0.75	0.79
Molecular weight	0.8	0.87
Drug likeness	0.39	0.96
No risk of mutagenicity	1.0	0.8
No risk of tumorigenicity	1.0	1.0
No risk of irritating effect	1.0	1.0
No risk of reproductive effect	1.0	1.0

hydrophilicity of both compounds. It has been suggested that high log P value is associated with poor absorption or permeation and it must be less than 5. This study suggested that both the compounds confirmed to this limit, and NCI140052 has better log P value than NCI295274. Typically, low solubility is associated with bad absorption, so the general aim is to avoid poorly soluble compounds. The aqueous solubility (log S) of a compound significantly affects its absorption and distribution characteristics. The predicted log S values of the studied compounds were within the acceptable limit. Drug score was calculated to judge the compound's overall potential as a drug candidate. It combines druglikeness, $c$log P, log S, molecular weight and toxicity risk parameters which are shown in Table 5. Drug score showed that NCI140052 has higher score of 0.956 compare to NCI295274 (0.39). This result further encourages us to discover newer PKB β inhibitors for the treatment of cancer.

4. Conclusions

In this study, we described a rational strategy for the identification of novel PKB β inhibitors using combined pharmacophore-based virtual screening along with docking and *in silico* pharmacokinetic and toxicity studies. The best pharmacophore model was established using DISCOtech and GASP module and was validated through ROC and GH scoring methods. The best pharmacophore model was further employed as a 3D search query to screen NCI database. Ten (10) molecules were chosen based on Q_{fit} value of more than 95 for molecular docking study along with three known PKB β inhibitors. Molecular docking study was performed to improve the reliability and accuracy of virtual screening. Then, two preferable hits based on the best docking score were selected for *in silico* pharmacokinetic and toxicities. Results of *in silico* pharmacokinetic and toxicity study showed good pharmacokinetic properties. Hence, it was concluded that combination of the above modeling methods is able to identify new hits from chemical databases which may be a good lead to develop novel PKB β inhibitors for the treatment of cancer.

Acknowledgement

Appendix A. Supplementary data

Supplementary data associated with this article can be found, in the online version, at http://dx.doi.org/10.1016/j.jmgm.2013.01.010.

References

[1] B.T. Hennessy, D.L. Smith, P.T. Ram, Y. Lu, G.B. Mills, Exploiting the PI3K/AKT pathway for cancer drug discovery, Nature Reviews Drug discovery 4 (2005) 988–1004.

[2] A. Carnero, C.B. Aparicio, O. Renner, W. Link, J.F.M. Leal, The PTEN/PI3K/AKT signalling pathway in cancer, therapeutic application, Current Cancer Drug Targets 8 (2008) 187–198.

[3] M.P. Scheid, J.R. Woodgett, Unravelling the activation mechanisms of protein kinase B/Akt, FEBS Letters 546 (2003) 108–112.

[4] C.C. Milburn, M. Deak, S.M. Kelly, N.C. Price, D.R. Alessi, D.M.F.V. Aalten, Binding of phoisphatidylinositol 3,4,5-trisphosphate to the pleckstrin homology domain of protein kinase B induces a conformational change, Journal of Biochemistry 375 (2003) 531–538.

[5] D.D. Sarbassov, D.A. Guertin, S.M. Ali, D.M. Sabatini, Phosphorylation and regulation of Akt/PKB by the rictor-mTOR complex, Science 307 (2005) 1098–1101.

[6] J.R. Testa, A. Bellacosa, AKT plays a central role in tumorigenesis, Proceedings of the National Academy of Sciences of the United States of America 98 (2001) 10983–10985.

[7] I. Vivanco, C. Sawyers, The phosphatidylinositol 3-kinase AKT pathway in human cancer, Nature Reviews Cancer 2 (2002) 489–501.

[8] E.M. Sale, G.J. Sale, Protein kinase B: signalling roles and therapeutic targeting, Cellular and Molecular Life Sciences 65 (2008) 113–127.

[9] I. Collins, Targeted small molecule inhibitors of protein kinase B as anticancer agents, Anti-Cancer Agents in Medicinal Chemistry 9 (2009) 32–50.

[10] D. Mahadevan, G. Powis, E.A. Mash, B. George, V.M. Gokhale, S. Zhang, K. Shakalya, L. Du-Cuny, M. Berggren, M.A. Ali, U. Jana, N. Ihle, S. Moses, C. Franklin, S. Narayan, N. Shirahatti, E.J. Meuillet, Discovery of a novel class of AKT pleckstrin homology domain inhibitors, Molecular Cancer Therapeutics 7 (2008) 2621–2632.

[11] C.W. Lindsley, S.F. Barnett, M. Yaroschak, M.T. Bilodeau, M.E. Layton, Recent progress in the development of ATP-competitive and allosteric Akt kinase inhibitors, Current Topics in Medicinal Chemistry 7 (2007) 1349–1363.

[12] C.W. Lindsley, Z. Zhao, W.H. Leister, R.G. Robinson, S.F. Barnett, D. Defeo-Jones, R.E. Jones, G.D. Hartman, J.R. Huff, H.E. Huber, M.E. Duggan, Allosteric Akt (PKB) inhibitors: discovery and SAR of isoenzyme specificity, Bioorganic and Medicinal Chemistry Letters 15 (2005) 761–764.

[13] Q. Li, T. Li, G. Zhu, J. Gong, A. Claibone, C. Dalton, Y. Luo, E.F. Johnson, Y. Shi, X. Liu, V. Klinghofer, J.L. Bauch, K.C. Marsh, J.J. Bousk, S. Arries, R. de Jong, T. Oltersdorf, V.S. Stoll, C.G. Jakob, S.H. Rosenberg, V.L. Giranda, Discovery of trans-3,4′-bispyridinylethylenes as potent and novel inhibitors of protein kinase B (PKB/Akt) for the treatment of cancer: synthesis and biological evaluation, Bioorganic and Medicinal Chemistry Letters 16 (2006) 1679–1685.

[14] G. Zhu, J. Gong, A. Claiborne, K.W. Woods, V.B. Gandhi, S. Thomas, Y. Luo, X. Liu, Y. Shi, R. Guan, S.R. Magnone, V. Klinghofer, E.F. Johnson, J. Bouska, A. Shoemaker, A. Oleksijew, V.S. Stoll, R. de Jong, T. Oltersdorf, Q. Li, S.H. Rosenberga, V.L. Giranda, Isoquinoline–pyridine-based protein kinase B/Akt antagonists: SAR and in vivo antitumor activity, Bioorganic and Medicinal Chemistry Letters 16 (2006) 3150–3155.

[15] K.W. Woods, J.P. Fischer, A. Claiborne, T. Li, S.A. Thomas, G. Zhu, R.B. Diebold, X. Liu, Y. Shi, V. Klinghofer, E.K. Han, R. Guan, S.R. Magnone, E.F. Johnson, J.J. Bouska, A.M. Olson, R. de Jong, T. Oltersdorf, Y. Luo, S.H. Rosenberg, V.L. Giranda, Q. Li, Synthesis and SAR of indazole-pyridine based protein kinase B/Akt inhibitors, Bioorganic and Medicinal Chemistry Letters 14 (2006) 6832–6848.

[16] S. Ajmani, A. Agrawal, S. kulkarni, A comprehensive structure–activity analysis of protein kinase B-alpha (Akt1) inhibitors, Journal of Molecular Graphics and Modelling 28 (2010) 683–694.

[17] H. Chen, T. Tsalkova, F.C. Mei, Y. Hua, X. Cheng, J. Zhou, 5-Cyano-6-oxo-1,6-dihydro-pyrimidines as potent antagonists targeting exchange proteins directly activated by cAMP, Bioorganic and Medicinal Chemistry Letters 22 (2012) 4038–4043.

[18] G. Zhu, J. Gong, V.B. Gandhi, K. Woods, Y. Luo, X. Liu, R. Guan, V. Klinghofer, E.F. Johnson, V.S. Stoll, M. Mamo, Q. Li, S.H. Rosenberg, V.L. Giranda, Design and synthesis of pyridine-pyrazolopyridine-based inhibitors of protein kinase B/Akt, Bioorganic and Medicinal Chemistry Letters 15 (2007) 2441–2452.

[19] D.A. Heerding, N. Rhodes, J.D. Leber, T.J. Clark, R.M. Keenan, L.V. Lafrance, M. Li, I.G. Safonov, D.T. Takata, J.W. Venslavsky, D.S. Yamashita, A.E. Choudhry, R.A. Copeland, Z. Lai, M.D. Schaber, P.J. Tummino, S.L. Strum, E.R. Wood, D.R. Duckett, D. Eberwein, V.B. Knick, T.J. Lansing, R.T. McConnell, S. Zhang, E.A. Minthorn, N.O. Concha, G.L. Warren, R. Kumar, Identification of 4-(2-(4-amino-1,2,5-oxadiazol-3-yl)-1-ethyl-7-{[(3S)-3-piperidinylmethyl]oxy}-1H-imidazo[4,5-c]pyridin-4-yl)-2-methyl-3-butyn-2-ol (GSK690693), a novel inhibitor of AKT kinase, Journal of Medicinal Chemistry 51 (2008) 5663–5679.

[20] Kh.D. Singh, M. Karthikeyan, P. Kirubakaran, S. Nagamani, Pharmacophore filtering and 3D-QSAR in the discovery of new JAK2 inhibitors, Journal of Molecular Graphics and Modelling 30 (2011) 186–197.

[21] A.H. Al-Nadafa, M.O. Taha, Discovery of new renin inhibitory leads via sequential pharmacophore modeling, QSAR analysis, in silico screening and in vitro evaluation, Journal of Molecular Graphics and Modelling 29 (2011) 843–864.

[22] X. Dong, J. Yan, L. Du, P. Wu, S. Huang, T. Liu, Y. Hu, Pharmacophore identification, docking and "in silico" screening for novel CDK1 inhibitors, Journal of Molecular Graphics and Modelling 37 (2012) 77–86.

[23] X. Dong, X. Zhou, H. Jing, J. Chen, T. Liu, B. Yang, Q. He, Y. Hu, Pharmacophore identification, virtual screening and biological evaluation of prenylated flavonoids derivatives as PKB/Akt1 inhibitors, European Journal of Medical Chemistry 46 (2011) 5949–5958.

[24] P. Purushottamachar, J.B. Patel, L.K. Gediya, O.O. Clement, V.C.O. Njar, First chemical feature-based pharmacophore modeling of potent retinoidal retinoic acid metabolism blocking agents (RAMBAs): identification of novel RAMBA scaffolds, European Journal of Medicinal Chemistry 47 (2012) 412–423.

[25] D. Butina, M.D. Segall, K. Frankcombe, Predicting ADME properties *in silico*: methods and models, Drug Discovery Today 11 (2002) 583–588.

[26] T. McHardy, J.J. Caldwell, K.M. Cheung, L.J. Hunter, K. Taylor, M. Rowlands, R. Ruddle, A. Henley, A.H. Brandon, M. Valenti, T.G. Davies, L. Fazal, L. Seavers, F.I. Raynaud, S.A. Eccles, G.W. Aherne, M.D. Garrett, I. Collins, Discovery of 4-amino-1-(7*H*-pyrrolo[2,3-*d*]pyrimidin-4-yl)piperidine-4-carboxamides as selective orally active inhibitors of protein kinase B (Akt), Journal of Medicinal Chemistry 53 (2010) 2239–2249.

[27] J.J. Caldwell, T.G. Davies, A. Donald, T. McHardy, M.G. Rowlands, G.W. Aherne, L.K. Hunter, K. Taylor, R. Ruddle, F.I. Raynaud, M. Verdonk, P. Workman, M.D. Garrett, I. Collins, Identification of 4-(4-aminopiperidin-1-yl)-7*H*-pyrrolo[2,3-*d*]pyrimidines as selective inhibitors of protein kinase B through fragment elaboration, Journal of Medicinal Chemistry 51 (2008) 2147–2157.

[28] A. Donald, T. McHardy, M.G. Rowlands, L.J.K. Hunter, T.G. Davies, V. Berdini, R.G. Boyle, G.W. Aherne, M.D. Garrett, I. Collins, Rapid evolution of 6-phenylpurine inhibitors of protein kinase B through structure-based design, Journal of Medicinal Chemistry 50 (2007) 2289–2292.

[29] Tripos Associates, SYBYL X Molecular Modeling Software, Version 1.2, St. Louis, MO, 2011, http://www.tripos.com

[30] J. Gasteiger, M. Marsili, Iterative partial equalization of orbital electronegativity – a rapid access to atomic charges, Tetrahedron 36 (1980) 3219–3228.

[31] M. Clark, R.D. Cramer III, N.V. Opdenbosch, Validation of the general purpose Tripos 5.2 forcefield, Journal of Computational Chemistry 10 (1989) 982–1012.

[32] H. Yuan, P.A. Petukhov, Improved 3D-QSAR CoMFA of the dopamine transporter blockers with multiple conformations using the genetic algorithm, Bioorganic and Medicinal Chemistry Letters 16 (2006) 6267–6272.

[33] T. Fawcett, An introduction to ROC analysis, Pattern Recognition Letters 27 (2006) 861–874.

[34] O.F. Güner, Metric for analyzing hit lists pharmacophores, in: O.F. Güner (Ed.), Pharmacophore Perception, Development, and Use in Drug Design, International University Line, La Jolla, CA, 2000, pp. 191–211.

[35] O.F. Güner, Strategies for database mining and pharmacophore development, in: O.F. Guner (Ed.), Pharmacophore Perception, development, and Use in Drug Design, International University Line, La Jolla, CA, 2000, pp. 213–236.

[36] J.M. Yang, T.W. Shen, A pharmacophore-based evolutionary approach for screening selective estrogen receptor modulators, PROTEINS: Structure, Function, and Bioinformatics 59 (2005) 205–220.

[37] I. Muegge, Selection criteria for drug-like compounds, Medicinal Research Reviews 23 (2003) 302–321.

[38] T.G. Davies, M.L. Verdonk, B. Graham, S. Saalau-Bethell, C.C. Hamlett, T. McHardy, I. Collins, M.D. Garrett, P. Workman, S.J. Woodhead, H. Jhoti, D. Barford, A structural comparison of inhibitor binding to PKB, PKA and PKA–PKB chimera, Journal of Molecular Biology 367 (2007) 882–894.

[39] http://www.organic-chemistry.org/prog/peo, November, 2012.